Research in Astron. Astrophys. **2013** Vol. **13** No. **5**, 593–603
http://www.raa-journal.org *http://www.iop.org/journals/raa*

***R**esearch in*
***A**stronomy and*
***A**strophysics*

The refined physical parameters of transiting exoplanet system HAT-P-24 *

Xiao-Bin Wang[1,2], Sheng-Hong Gu[1,2], Andrew Collier Cameron[3], Hong-Bo Tan[1,4], Ho-Keung Hui[5], Chi-Tai Kwok[5], Bill Yeung[6] and Kam-Cheung Leung[6]

[1] National Astronomical Observatories / Yunnan Observatory, Chinese Academy of Sciences, Kunming 650011, China; *shenghonggu@ynao.ac.cn*
[2] Key Laboratory for the Structure and Evolution of Celestial Objects, Chinese Academy of Sciences, Kunming 650011, China
[3] School of Physics and Astronomy, University of St Andrews, North Haugh, St Andrews, Fife KY16 9SS UK
[4] University of Chinese Academy of Sciences, Beijing 100049, China
[5] Hokoon Nature Education cum Astronomical Centre, Sik Sik Yuen, Hong Kong, China
[6] Hong Kong Astronomical Society, Hong Kong, China

Received 2012 November 18; accepted 2012 December 23

Abstract The transiting exoplanet system HAT-P-24 was observed by using CCD cameras at Yunnan Observatory and Hokoon Astronomical Centre, China in 2010 and 2012. In order to enhance the signal to noise ratio of transit events, the observed data are corrected for systematic errors according to Collier Cameron et al.'s coarse decorrelation and Tamuz et al.'s SYSREM algorithms. Three new complete transit light curves are analyzed by means of the Markov chain Monte Carlo technique, and the new physical parameters of the system are derived. They are consistent with the old ones from the discovered paper except for a new larger radius $R_{\rm p} = 1.364\,R_{\rm J}$ of HAT-P-24b, which confirms its inflated nature. By combining the five available epochs of mid-transit derived from complete transit light curves, the orbital period of HAT-P-24b is refined to $P = 3.3552479$ d and no obvious transit timing variation signal can be found from these five transit events during 2010–2012.

Key words: exoplanet system — transit — individual: HAT-P-24

1 INTRODUCTION

Knowledge of exoplanet systems has been greatly expanded through the study of transiting exoplanets during recent years. Photometric observations of transiting exoplanets can provide us with the sizes and masses of these planets, which are important for understanding their formation and evolution (Charbonneau et al. 2000). The continued monitoring of previously discovered transiting exoplanets can signify whether there are some other planets in the same system, through analyzing transit timing variation (TTV) and transit duration variation (TDV) (Agol et al. 2005; Holman &

* Supported by the National Natural Science Foundation of China.

Murray 2005; Kipping 2009a,b). Furthermore, new observations can allow us to improve measurements of the physical parameters associated transiting systems, which are helpful for investigating which factors are related to exoplanet composition, structure and evolution. Therefore, photometric follow-up observations of known exoplanet systems are also very important in addition to discovering new ones by photometric surveys. Since 2007, we have begun a monitoring project for known transiting exoplanet systems by using the 1 m telescope at Yunnan Observatory and the 50 cm telescope at Hokoon Astronomical Centre. The goals are modeling the TTV or TDV phenomena and refining the physical parameters associated with the selected exoplanet systems.

HAT-P-24b was discovered by Kipping et al. (2010), and it is an inflated hot Jupiter with a mass of $0.681\,M_{\rm J}$, a radius of $1.243R_{\rm J}$ and a small eccentricity of $e = 0.052$. The host star GSC 0774–01441 has spectral type F8V and brightness $V = 11.818$. We monitored this system at Yunnan Observatory, China in 2010 and 2012, and at Hokoon Astronomical Centre, Hong Kong, China in 2010, and three complete transit light curves were obtained. Here, we present the relative analysis results on the HAT-P-24 system, which are based on our new photometric observations and the radial velocity observations in the literature (Kipping et al. 2010). In Section 2, we describe the photometric observations and relative data reduction strategy. In Section 3, the parameter analysis is performed using the technique of Markov chain Monte Carlo (MCMC) and we improve the orbital period by linear fitting to epochs of mid-transit. In Section 4, the new results are discussed. Finally, we give a summary of our new study in Section 5.

2 OBSERVATIONS AND DATA REDUCTION

2.1 Photometric Observations with the 1 m Telescope

HAT-P-24 was observed using an Andor CCD camera with a 2k×2k chip attached to the 1 m telescope at Yunnan Observatory, China on 2010 Dec. 28 and 2012 Mar. 15. During all observations, an R filter was used and the field of view was $7.3'$. In the first observing run in 2010, the weather was clear with good seeing conditions and the status of the instrument was also fine. During the second observing run in 2012, the weather was clear, but the seeing conditions were bad, and the status of the instrument was also not good. The tracking of the telescope was slightly bad, and there was some dust on the filter and the window of the CCD detector, so we used a longer exposure time than on the first run to obtain higher CCD counts for the stars. Detailed information on observations is summarized in Table 1.

2.2 Photometric Observations with the 50 cm Telescope

We observed HAT-P-24 by means of an Apogee CCD camera with a 3k×3k chip attached to the 50 cm telescope at the Hokoon Astronomical Centre, Hongkong, China on 2010 Dec. 28, which is the same night as the first run at Yunnan Observatory, namely, we used two facilities to observe the same transit event of HAT-P-24. In this observing run, an R filter was employed and the field of view was $31.4'$. The weather was good for photometric observations despite the heavy light pollution in the Hong Kong area. The observing log is listed in Table 1.

Table 1 The Observing Log of the Transiting Exoplanet System HAT-P-24

Date	Telescope	Filter	Exposure time (s)	Number of points	Precision (mag)
2010.12.28	YO1 m	R	90–120	197	0.00165
2012.03.15	YO1 m	R	150	99	0.00250
2010.12.28	HK50 cm	R	60	321	0.00283

2.3 Data Reduction

The observed CCD images of both instruments are reduced in the standard way by means of the IRAF package, including image trimming, bias subtraction, dark current subtraction, flat-field correction and cosmic ray removal. During this procedure, after trimming, we use multiple frames of bias, dark current, and flat-field to produce the corresponding master bias, dark current, and flat-field images, respectively, which are used in the related steps of image reduction. Values of the instrumental magnitude for the target star and comparison stars in the reduced images are measured by using the APPHOT sub-package in IRAF. In the measurements, an optimal aperture is selected for each dataset so as to get the minimum dispersion for the observed light curve. Due to the different quality of CCD images taken in two nights at Yunnan Observatory, 15 and 9 comparison stars are selected to model the systematic errors in photometric data on 2010 Dec. 28 and 2012 Mar. 15, respectively, although we chose the same field of view for both observing runs. For the data taken at the Hokoon Astronomical Centre, we select 28 comparison stars due to the large field of view of the 50 cm telescope.

2.4 Systematic Error Correction

Because the transit signal of an exoplanet is normally weak, we use coarse de-correlation and SYSREM methods to correct the systematic errors in the photometric data so as to enhance the signal to noise ratio of transit events (Collier Cameron et al. 2006; Tamuz et al. 2005). Firstly, the photometric data of all comparison stars in the CCD images are iteratively analyzed by the coarse de-correlation method, during which the possible variable objects and the objects with low precision are identified. Secondly, the stable comparison stars with higher precision are used to model the systematic errors in the photometric data with the SYSREM method. Then, photometric data of the target star, HAT-P-24, are corrected by these modeled systematic errors. Because we model the systematic errors by simply using the stable comparison stars, a process which does not consider systematic trends for the target star HAT-P-24, there are still systematic trends left in the resulting light curves of the target HAT-P-24. Thus, we use a straight line to fit the two regions outside of the transit event for each dataset, so that we can correct the data for a linear systematic trend. For the time system of our new photometric data, we convert the local time to the Barycentric Julian date under the Coordinated Universal Time ($\mathrm{BJD_{UTC}}$) which is used widely in the study of exoplanetary systems. Through the above steps, we have derived the final light curves of the transit events for the system HAT-P-24, which are displayed in Figure 1 and are used to obtain physical parameters of the planetary system in the next section.

3 LIGHT CURVE ANALYSIS

In order to derive the system parameters of HAT-P-24, we use the MCMC technique (details can be found in references: Collier Cameron et al. 2007; Pollacco et al. 2008; Enoch et al. 2010) to simultaneously estimate the photometric model of an exoplanet transit event and the radial velocity model of the host star's orbital motion with three transit light curves and published radial velocity curve (Kipping et al. 2010, see table 1 of that paper). Since the work of Pollacco et al. (2008), the code we used has been updated to work with cases of both circular and eccentric orbits; the adjusted parameters are $\{T_0, P, \Delta F, t_{\mathrm{T}}, b, M_*, K_1, e, \omega\}$, T_0 is the epoch of mid-transit, P is the orbital period, ΔF is the fractional flux deficit during the transit when not considering the stellar limb-darkening, t_{T} is the transit duration from the first contact to the fourth one, b is the impact parameter, M_* is the mass of the host star, K_1 is the semi-amplitude of the radial velocity curve of the host star, e is the orbital eccentricity and ω is the argument of periastron. Later, Enoch et al. (2010) established a new calibration for the mass of a host star based on stellar effective temperature T_{eff}, metallicity [Fe/H] and stellar density ρ_*, and put it in the recent modified version of the above

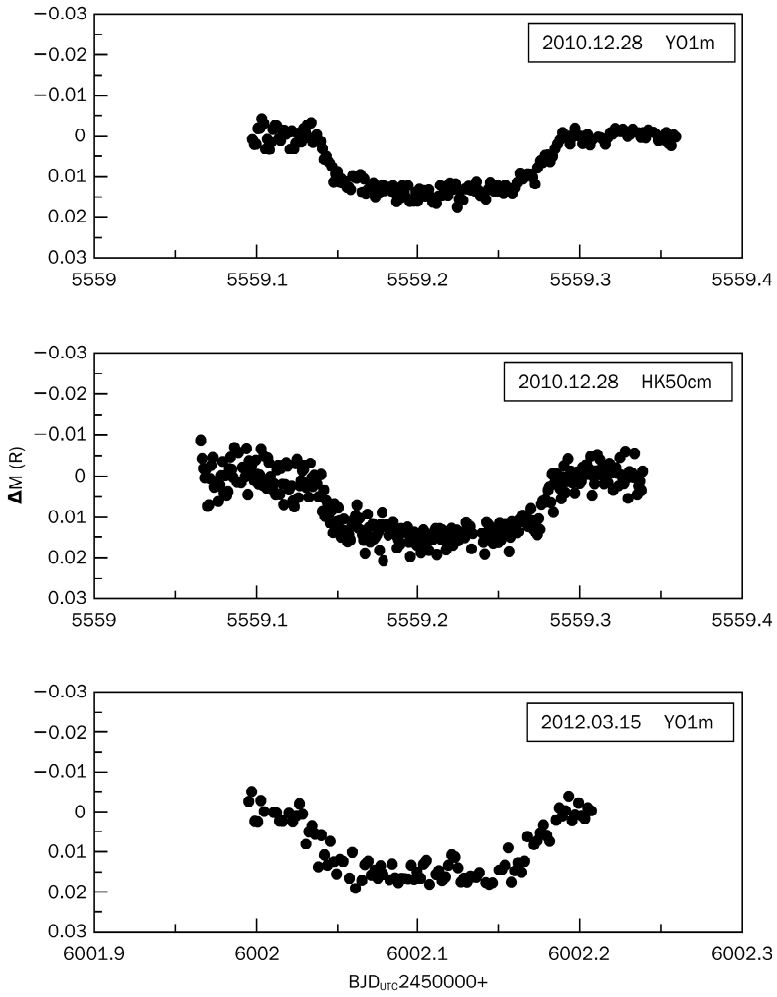

Fig. 1 The unbinned light curves of transit events of HAT-P-24b after adjustments for systematic error and trend corrections.

code. Therefore, the mass of the host star M_* is not a free parameter, but rather is calculated with Enoch et al. (2010)'s calibration. In practice, the proposal parameters are changed to $\{T_0,\, P,\, \Delta F,\, t_{\rm T},\, b,\, K_1,\, e\cos\omega,\, e\sin\omega\}$. Using $e\cos\omega$ and $e\sin\omega$ instead of e and ω as the jump parameters, we increase the convergence rate for the planetary system with small eccentricity. This aspect is clearly explained in the work of Ford (2005).

The transit light curve is modeled using a small planet approximation (Mandel & Agol 2002), and the 4-coefficient limb-darkening law is used (Claret 2000). The four limb-darkening coefficients are calculated from Claret (2000)'s table of the R band through interpolation according to the effective temperature $T_{\rm eff}$, surface gravity $\log g$, and metallicity [Fe/H] of the host star. With the Metropolis-Hastings algorithm, the posterior probability distributions of the system parameters are obtained, from which the best values and uncertainties of the parameters are derived. During the calculation, the effective temperature $T_{\rm eff} = 6373$ K and metallicity [Fe/H]$= -0.16$ of the host star are adopted from Kipping et al. (2010)'s work.

3.1 Initial MCMC Analysis

First of all, we have simultaneously analyzed three new transit light curves and Kipping et al. (2010)'s radial velocity curve to derive a global solution for photometric and radial velocity observations. The input values of some system parameters for MCMC analysis are adopted from the results of Kipping et al. (2010); the jumping step lengths of the parameters are initially set by considering the published uncertainties of the parameters, and are adjusted according to the acceptance ratio. During the calculation, we have tried different chain lengths from 10^4 to 10^5 and the results are almost the same as each other. This indicates that, for our case, it is not necessary to use a longer chain in order to derive a convergent solution. Actually, we have calculated a few of the 10^4 MCMC chains with somewhat different initial parameter sets, and almost the same posterior probability distributions were obtained. This gives an orbital period of $P = 3.35524825$ d, which can fit our new photometric observations and Kipping et al. (2010)'s radial velocity observations well. In the second step, we set the orbital period value as above so we can use the transit model to derive accurate values for the epochs of mid-transit. With the MCMC procedure, we have analyzed the individual transit light curve to get the epoch of mid-transit for each transit event, which is shown in Table 2. By combining the new epochs of mid-transit with the ones collected from the literature, study of the orbital period for HAT-P-24 will be performed in the next sub-section.

3.2 Orbital Period Study

In order to obtain an accurate value of orbital period, we collect all available epochs of mid-transit with higher precision for the HAT-P-24 system from the literature and the web, which are determined by using complete transit light curves with higher quality. An epoch of mid-transit with good precision is found in the Exoplanet Transit Database (ETD)[1] and a precise epoch of mid-transit based on their unique complete transit light curve is selected from Kipping et al. 2010's paper. These are listed in Table 2. Combining these two epochs of mid-transit with our three new ones, the orbital period study of the transiting system HAT-P-24 is conducted using a linear fitting. The newly derived linear ephemeris formula is as follows: $\mathrm{BJD_{UTC}}$=2455243.81797(78)+3.3552479(62)$\times E$. Here E represents the orbital cycles. The relative $(O-C)$ diagram is displayed in Figure 2. The epoch of mid-transit from Kipping et al. (2010) is used as the zero point for the new linear ephemeris formula.

Table 2 The Available Epochs of Mid-transit for HAT-P-24

T_0 (d) $\mathrm{BJD_{UTC}}$2450000+	Cycle	$(O-C)$ (d)	Source
5243.81878	0	0.00081	Kipping et al. (2010)
5559.21070	94	–0.00057	This paper
5559.21006	94	–0.00121	This paper
5599.47471	106	0.00046	ETD
6002.10454	226	0.00054	This paper

3.3 Final MCMC Analysis

In the above sub-section, we have derived a new accurate orbital period for the system HAT-P-24 through the $(O-C)$ analysis, which is the best way to determine the orbital period of an exoplanetary system. Now, we set the orbital period as this new value, and then perform the MCMC calculation to derive the physical parameters of the system HAT-P-24, based on three new transit light curves

[1] *http://var2.astro.cz/ETD/*

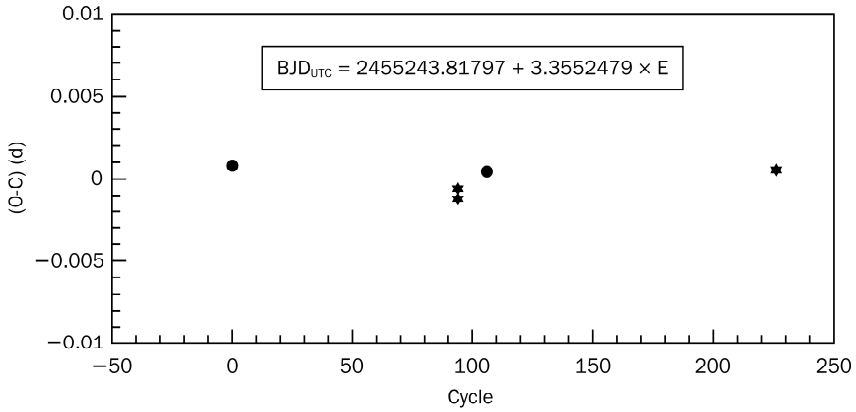

Fig. 2 The $(O-C)$ diagram for the orbital period study of the HAT-P-24 system. The star indicates our new epochs of mid-transit.

Table 3 System Parameters and 1σ Error Limits Derived from the MCMC Analysis

Parameter	Symbol	Value	Unit
Transit epoch	T_0	$\mathrm{BJD_{UTC}}$2455629.67053±0.00034	d
Orbital period	P	3.3552479±0.0000062	d
Planet/star area ratio	$(R_\mathrm{p}/R_*)^2$	0.01129±0.00016	
Transit duration	t_T	0.1535±0.0022	d
Impact parameter	b	$0.2367^{+0.0845}_{-0.0875}$	R_*
Stellar reflex velocity	K_1	83.2±3.3	m s^{-1}
Center-of-mass velocity	γ	$-0.37^{+0.24}_{-0.26}$	m s^{-1}
Orbital eccentricity	e	$0.064^{+0.023}_{-0.020}$	
Longitude of periastron	ω	$-125.39^{+287.73}_{-37.56}$	degree
Eccentricity×cos ω	$e\cos\omega$	$-0.0516^{+0.0191}_{-0.0192}$	
Eccentricity×sin ω	$e\sin\omega$	$-0.0131^{+0.0377}_{-0.0409}$	
Orbital inclination	i	$88.217^{+0.716}_{-0.693}$	degree
Orbital semi-major axis	a	$0.04655^{+0.00016}_{-0.00015}$	AU
Stellar mass	M_*	1.195±0.012	$M_\odot$
Stellar radius	R_*	1.321±0.063	$R_\odot$
Stellar density	ρ_*	$0.519^{+0.077}_{-0.062}$	$\rho_\odot$
Planet radius	R_p	1.364±0.068	R_J
Planet mass	M_p	0.691±0.027	M_J
Planet density	ρ_p	$0.272^{+0.044}_{-0.037}$	ρ_J
Planet temperature	T_eq	1637^{+35}_{-37}	K
Photometry χ^2/data points	$\chi^2_\mathrm{phot}/N_\mathrm{phot}$	611.6/617	
Radial velocity χ^2/data points	$\chi^2_\mathrm{RV}/N_\mathrm{RV}$	17.3/18	

and the radial velocity curve of Kipping et al. (2010). Here, we would like to mention that the radial velocity jitter of 7.4 m s^{-1} introduced by Kipping et al. (2010) is used for the radial velocity curve in our MCMC analysis. In the course of the calculation, we have done several 10^4 chain calculations to ensure that the posterior probability distribution samples converge to the stationary ones. Based on

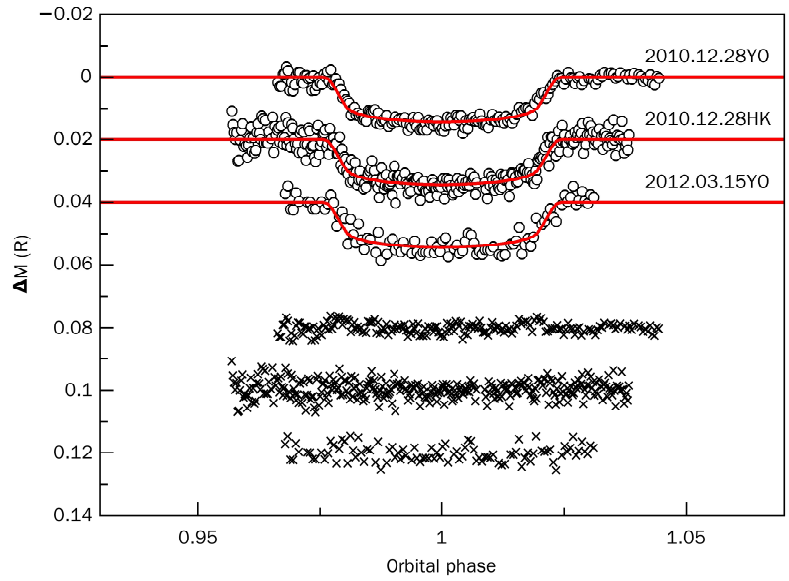

Fig. 3 Observed light curves and related model fitting. The circles represent the individual observation, the solid line represents the model and the cross represents the residual between the observation and model. For the sake of clarity, two light curves and the residuals between observations and the theoretical curve for each dataset are offset by constants while one is in the original form.

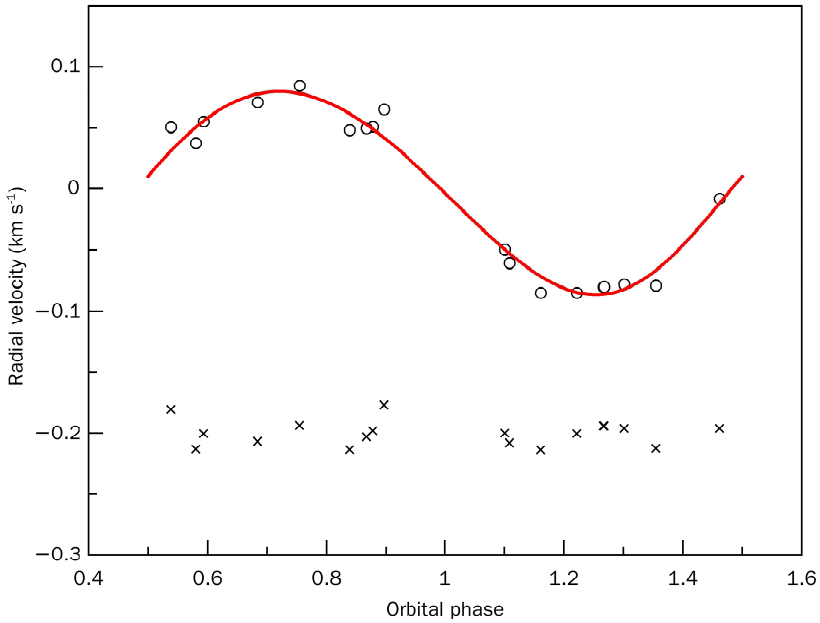

Fig. 4 Radial velocity curve and relative model fitting. The symbols are the same as in Fig. 3. For the sake of clarity, the residuals between observations and a theoretical curve are offset by a constant.

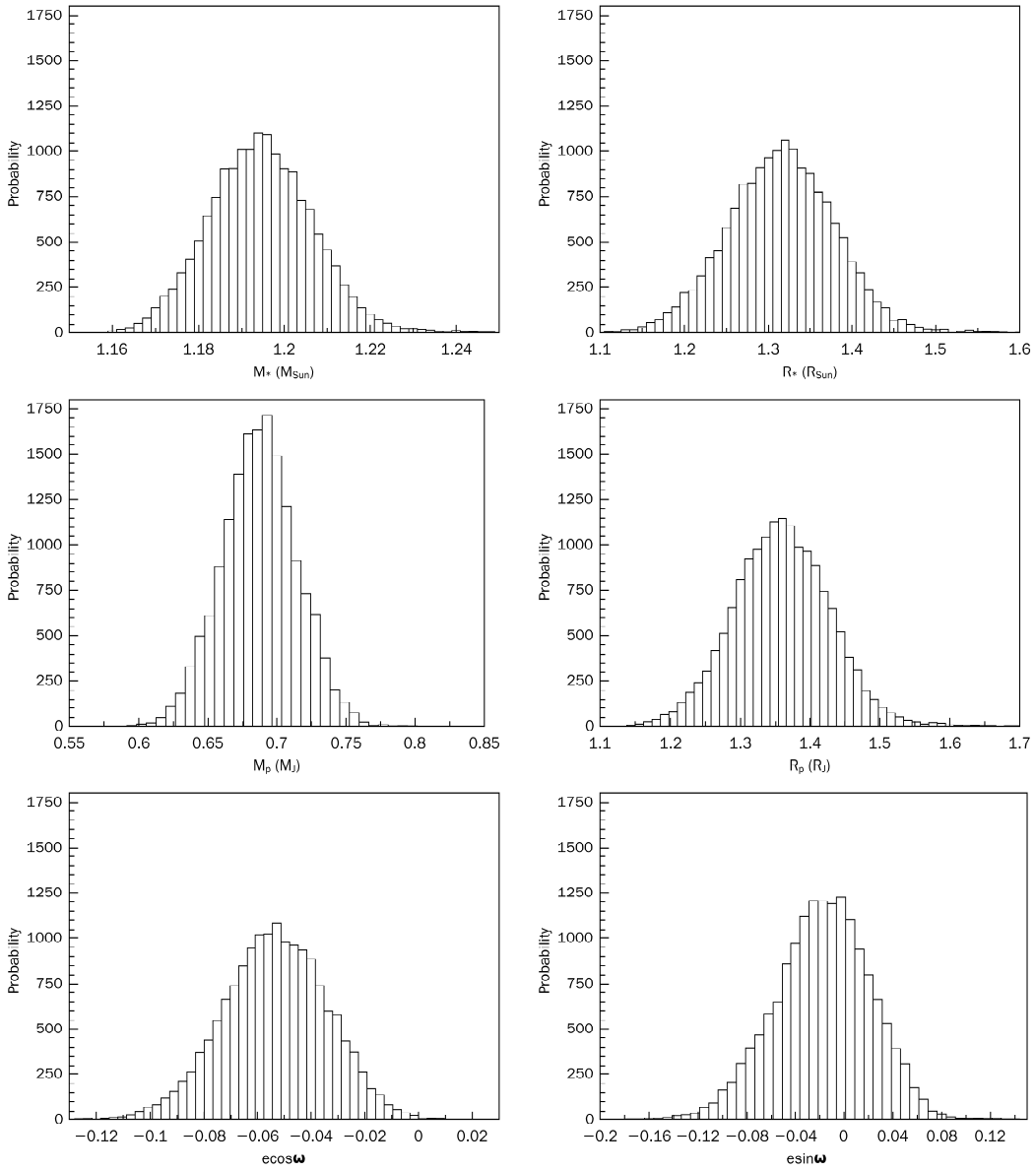

Fig. 5 The posterior probability distributions of some physical parameters describing HAT-P-24.

the posterior probability distributions, the best values of the system parameters are derived from their median values, and the uncertainties of the system parameters are taken as 1σ limits of the parameter spaces. The adopted values and their uncertainties are listed in Table 3 where the χ^2 and the number of data points are also given for photometry and radial velocity observations in the last two lines, and the relative model fitting is illustrated in Figures 3 and 4. The posterior probability distributions of six main physical parameters describing the HAT-P-24 system are displayed in Figure 5. It can be seen that all of these are very close to Gaussian distributions.

4 DISCUSSION

Based on the new photometric data and published radial velocity data, we have refined the physical parameters of the transiting exoplanetary system HAT-P-24 by using the MCMC technique. Comparing our results with those from Kipping et al. (2010) (their tables 4, 5 and 6), it can be seen that the new physical parameters of the HAT-P-24 system are almost consistent with the ones in the referenced paper, except for the radius of the planet. One point needs to be mentioned: the center-of-mass velocity γ listed in Table 3 is not the real center-of-mass velocity of the system. It just represents an arbitrary offset value in Keck radial velocity measurements (see details in the paper of Kipping et al. 2010).

Our new parameters describing the host star are very close to the ones from Kipping et al. (2010). The mass of $1.195\,M_{\odot}$ and the radius of $1.321R_{\odot}$ confirm the values $1.191\,M_{\odot}$ and $1.317R_{\odot}$ in Kipping et al. (2010)'s paper. This indicates that the mass of the host star derived by the calibration of Enoch et al. (2010) is very reliable when compared with the one based on isochrone analysis, which means that the new mass calibration of Enoch et al. (2010) is quite accurate.

For the planet HAT-P-24b, a small eccentricity $e = 0.064$ exists in the orbit, which is identical to the value of 0.067 given by Kipping et al. (2010)'s global modeling and is slightly larger than their refined value $e = 0.052$ (but is still consistent with each other considering the relative error bars). The mass of planet $0.691\,M_{\rm J}$ is quite close to that of $0.681\,M_{\rm J}$ in Kipping et al. (2010)'s paper, and the radius of planet $R_{\rm p} = 1.364R_{\rm J}$ is larger than their value $R_{\rm p} = 1.243R_{\rm J}$, which confirms it being an inflated planet.

The new orbital period is a little longer than the old one given by Kipping et al. (2010), and should be more accurate than the old one because the five epochs of mid-transit involved in the analysis are derived from the complete transit light curves with higher precision. In Kipping et al. (2010)'s work, they only had one complete transit light curve with high precision. From Figure 2, it is clear that the linear fitting to five epochs of mid-transit is good, and the rms of the $(O-C)$ values is 0.000861 d (74.4 s). Thus, no obvious TTV signal can be found from the presented $(O-C)$ analysis of orbital period. One point should be emphasized: as only five epochs of mid-transit with high precision are available up to now, this is not the time to give any conclusions on the TTV behavior of HAT-P-24.

The radius of $1.364R_{\rm J}$ is quite large when compared with the theoretical model of Fortney et al. (2007). We have compiled transiting exoplanet systems with similar planetary masses (the mass region represents $0.69\,M_{\rm J}$ of HAT-P-24b plus or minus its 1σ error limit of $0.03\,M_{\rm J}$) to HAT-P-24b from the literature. These are listed in Table 4. The values for the orbital semi-major axis

Table 4 The Transiting Systems with Similar Planetary Masses to HAT-P-24

Object	$M_{\rm p}$ ($M_{\rm J}$)	$R_{\rm p}$ ($R_{\rm J}$)	a (AU)	$a_{\odot}$ (AU)	Age (Gyr)	Reference
HAT-P-27/WASP-40b	0.660	1.038	0.0403	0.0534	4.4	Anderson et al. (2011) Béky et al. (2011)
Kepler-15b	0.66	0.96	0.05714	0.0632	3.7	Endl et al. (2011)
Kepler-6b	0.669	1.323	0.04567	0.0324	3.8	Dunham et al. (2010)
HAT-P-4b	0.68	1.27	0.0446	0.0272	4.2	Kovács et al. (2007)
HD209458b	0.686	1.347	0.04747	0.0366	4.5	Brown et al. (2001) Mazeh et al. (2000) Southworth (2010)
HAT-P-24b	0.691	1.364	0.04655	0.0291	2.8	This paper Kipping et al. (2010)
HAT-P-30/WASP-51b	0.711	1.340	0.0419	0.0293	1.0	Enoch et al. (2011) Johnson et al. (2011)
WASP-35b	0.72	1.32	0.04317	0.0360	5.01	Enoch et al. (2011)

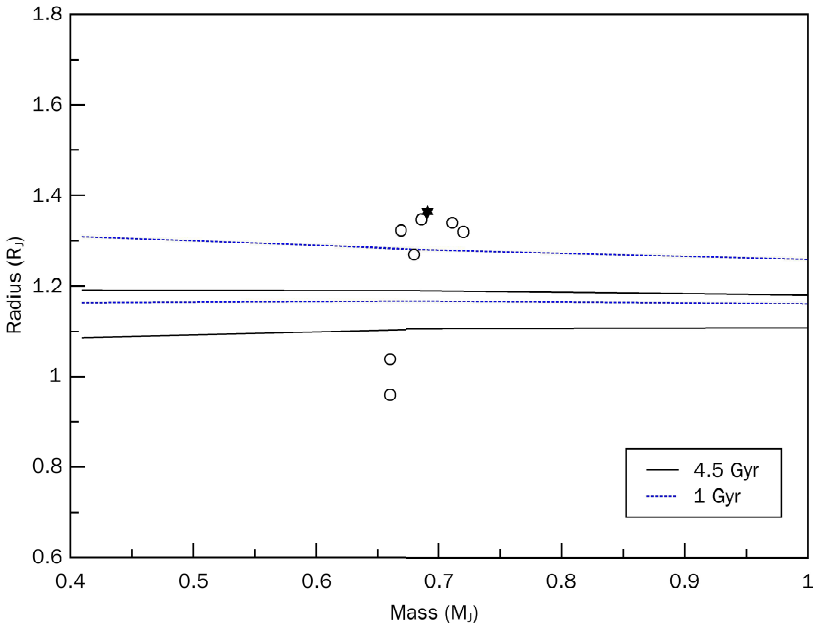

Fig. 6 The mass-radius relation diagram of HAT-P-24b (star) and exoplanets with similar masses. For each age, the upper lines represent the theoretical radii of planets at an orbital distance of 0.02 AU, whereas the lower lines represent the ones at an orbital distance of 0.045 AU.

(a) of these exoplanetary systems are scaled by using the relationship $a_{\odot}$=$a(L_{\odot}/L_{*})^{1/2}$, so that the measurements can be compared with theoretical models (Fortney et al. 2007). These systems were discovered by photometric surveys, including ground-based instruments and space missions. According to the theoretical results of Fortney et al. (2007) (tables 3 and 4 of their paper), we have produced a mass-radius diagram that includes the theoretical values at an orbital distance of 0.02 AU and 0.045 AU, and values of these selected exoplanets.

This diagram is shown in Figure 6, where four lines are given for the coreless planets (which have larger radii than the ones with core masses) at ages of 1 Gyr and 4.5 Gyr. In this diagram, we can see that only two of the samples are below the upper limits of the theoretical radii, and the other six exoplanets are above the theoretical values, which demonstrates that these six exoplanets are inflated. Among them, HAT-P-24b is the most inflated one in this mass region (0.66–0.72 $M_{\rm J}$). This supports Fortney et al. (2007)'s idea, that most hot Jupiters have larger radii due to additional energy sources.

5 SUMMARY

Based on the above analysis for the new photometric observations and published radial velocity data, we have derived new physical parameters describing the transiting system HAT-P-24. The new result is comparable with the old one (Kipping et al. 2010). The orbit shows a small eccentricity $e = 0.064$, which confirms the discovery of Kipping et al. (2010). The radius of planet $R_{\rm p} = 1.364 R_{\rm J}$ supports its inflated nature. The new, more accurate orbital period is $P = 3.3552479$ d, and no obvious TTV signal can be found from the presented ($O - C$) analysis of its orbital period.

Acknowledgements We thank the operators of the 1 m telescope and some graduate students at Yunnan Observatory for their support and help during our observations. This work was supported by

the National Natural Science Foundation of China (Grant No. 10873031), the Chinese Academy of Sciences (KJCX2-YW-T24), and a special grant from Sik Sik Yuen of Hong Kong, China.

References

Agol, E., Steffen, J., Sari, R., & Clarkson, W. 2005, MNRAS, 359, 567
Anderson, D. R., Barros, S. C. C., Boisse, I., et al. 2011, PASP, 123, 555
Béky, B., Bakos, G. Á., Hartman, J., et al. 2011, ApJ, 734, 109
Brown, T. M., Charbonneau, D., Gilliland, R. L., Noyes, R. W., & Burrows, A. 2001, ApJ, 552, 699
Charbonneau, D., Brown, T. M., Latham, D. W., & Mayor, M. 2000, ApJ, 529, L45
Claret, A. 2000, A&A, 363, 1081
Collier Cameron, A., Pollacco, D., Street, R. A., et al. 2006, MNRAS, 373, 799
Collier Cameron, A., Wilson, D. M., West, R. G., et al. 2007, MNRAS, 380, 1230
Dunham, E. W., Borucki, W. J., Koch, D. G., et al. 2010, ApJ, 713, L136
Endl, M., MacQueen, P. J., Cochran, W. D., et al. 2011, ApJS, 197, 13
Enoch, B., Collier Cameron, A., Parley, N. R., & Hebb, L. 2010, A&A, 516, A33
Enoch, B., Anderson, D. R., Barros, S. C. C., et al. 2011, AJ, 142, 86
Ford, E. B. 2005, AJ, 129, 1706
Fortney, J. J., Marley, M. S., & Barnes, J. W. 2007, ApJ, 659, 1661
Holman, M. J., & Murray, N. W. 2005, Science, 307, 1288
Johnson, J. A., Winn, J. N., Bakos, G. Á., et al. 2011, ApJ, 735, 24
Kipping, D. M. 2009a, MNRAS, 392, 181
Kipping, D. M. 2009b, MNRAS, 396, 1797
Kipping, D. M., Bakos, G. Á., Hartman, J., et al. 2010, ApJ, 725, 2017
Kovács, G., Bakos, G. Á., Torres, G., et al. 2007, ApJ, 670, L41
Mandel, K., & Agol, E. 2002, ApJ, 580, L171
Mazeh, T., Naef, D., Torres, G., et al. 2000, ApJ, 532, L55
Pollacco, D., Skillen, I., Collier Cameron, A., et al. 2008, MNRAS, 385, 1576
Southworth, J. 2010, MNRAS, 408, 1689
Tamuz, O., Mazeh, T., & Zucker, S. 2005, MNRAS, 356, 1466